

# Age-Associated Changes of Nitric Oxide Concentration Dynamics in the Central Nervous System of Fisher 344 Rats

Ana Ledo · Cátia F. Lourenço · Miguel Caetano ·  
Rui M. Barbosa · João Laranjinha

Received: 16 May 2014 / Accepted: 17 September 2014 / Published online: 2 October 2014  
© Springer Science+Business Media New York 2014

**Abstract** The increase in life expectancy is accompanied by an increased risk of developing neurodegenerative disorders and age is the most relevant risk factor for the appearance of cognitive decline. While decreased neuronal count has been proposed to be a major contributing factor to the appearance of age-associated cognitive decline, it appears to be insufficient to fully account for the decay in mental function in aged individuals. Nitric oxide ( $\bullet$ NO) is a ubiquitous signaling molecule in the mammalian central nervous system. Closely linked to the activation of glutamatergic transmission in several structures of the brain, neuron-derived  $\bullet$ NO can act as a neuromodulator in synaptic plasticity but has also been linked to neuronal toxicity and degenerative processes. Many studies have proposed that changes in the glutamate- $\bullet$ NO signaling pathway may be implicated in age-dependent cognitive decline and that the exact effect of such changes may be region specific. Due to its peculiar physical–chemical properties, namely hydrophobicity, small size, and rapid diffusion properties, the rate and pattern of  $\bullet$ NO concentration changes are critical determinants for the understanding of its bioactivity in the brain. Here we show a detailed study of how  $\bullet$ NO concentration dynamics change in the different regions of the brain of Fisher 344 rats (F344) during aging. Using microelectrodes inserted into the living brain of

anesthetized F344 rats, we show here that glutamate-induced  $\bullet$ NO concentration dynamics decrease in the hippocampus, striatum, and cerebral cortex as animals age. performance in behavior testing of short-term and spatial memory, suggesting that the impairment in the glutamate:nNOS pathway represents a functional critical event in cognitive decline during aging.

**Keywords** Nitric oxide · Aging · Fischer 344 rats · In vivo · Electrochemical detection

## Introduction

The extension of lifespan has been associated with an increased risk for neurodegenerative disorders, suggesting a putative link between chronological age and disorders of the central nervous system (CNS). In reality, age is the greatest risk factor for cognitive decline and Alzheimer's disease (the leading cause of dementia) in the elderly population. In humans, fMRI studies have revealed that differences in activity of the hippocampus and associated cortical regions may correlate with tilting the equilibrium from normal to pathological aging (Small et al. 2002).

The aging process, particularly with what concerns the CNS, can lead to relatively intact cognitive function or to dementia. During normal aging, morphological and functional changes of the brain are seen in terms of brain weight, protein quality, number of neurons, and concentration of enzymes responsible for the synthesis of neurotransmitters. As reviewed elsewhere (Bishop et al. 2010), major pathways which impact the aging process have been identified in the brain, including insulin/IGF-1 signaling, TOR signaling, mitochondrial function, sirtuins, and caloric intake.

---

A. Ledo · C. F. Lourenço · M. Caetano ·  
R. M. Barbosa · J. Laranjinha  
Center for Neuroscience and Cell Biology, Coimbra, Portugal

M. Caetano · R. M. Barbosa · J. Laranjinha (✉)  
Faculty of Pharmacy, University of Coimbra, Health Science  
Campus, Azinhaga de Santa Comba, 3000-548 Coimbra,  
Portugal  
e-mail: laranjin@ci.uc.pt

Nitric oxide ( $\bullet$ NO) is a small free radical messenger molecule produced by  $\bullet$ NO synthase (NOS), an enzyme that catalyzes the conversion of L-arginine to L-citrulline and  $\bullet$ NO. Although three isoforms of NOS have been unequivocally identified (Alderton et al. 2001), the neuronal isoform (nNOS or NOS I) has been shown to be pivotal in regulation of synaptic transmission (Garthwaite 2008). This isoform is anchored to the post-synaptic density, in particular to the N-methyl-D-aspartate-type glutamate receptor (NMDAR) via protein–protein interaction mediated by the scaffold protein post-synaptic density protein 95 (PSD-95) (Brenman et al. 1996; Christopherson et al. 1999) and, as such,  $\bullet$ NO production is tightly coupled to glutamate neurotransmission and neuronal excitability.

In the CNS,  $\bullet$ NO acts as a ubiquitous messenger molecule and is involved in several critical processes such as the regulation of neurotransmitter release, synaptic plasticity, and neuronal excitability, and thus is a key player in memory and learning mechanisms (Garthwaite 2008). Paradoxically, deregulation of  $\bullet$ NO bioactivity and availability has been proposed to contribute to aging and neurodegenerative processes (Law et al. 2001).

Many reports have shown the presence of  $\bullet$ NO and NOS in aging structures of the CNS, namely the cerebral cortex, cerebellum, amygdala, hippocampus, striatum, among others [reviewed in (Jung et al. 2012)]. However, the role played by  $\bullet$ NO in the pathology of chronological aging is far from being consensual in the literature. Reports range from excessive  $\bullet$ NO production associated with overproduction of reactive oxygen species by mitochondria (Poon et al. 2004) to descriptions of NOS-positive neurons showing selective resistance to death in pathologies such as Alzheimer's and Huntington's disease (Ferrante et al. 1985; Unger and Lange 1992; Benzing and Mufson 1995). Also, changes in NOS expression levels may have alternating significance as a function of the specific brain region analyzed.

The discrepancies regarding the role of  $\bullet$ NO during aging have thus far been based on indirect determination of either  $\bullet$ NO concentration or the level of NOS expression, with little or no data being shown regarding how the particular concentration dynamics associated to specific signaling pathways change in the aging brain. The change in pattern of  $\bullet$ NO production and removal in each brain region may be more elucidative in deciphering its participation in brain aging than NOS expression level.

Deciphering to role of  $\bullet$ NO in brain aging has been hindered by its elusive nature. In fact this free radical messenger is present in low nanomolar concentrations, has a short half-life and rapidly diffuses in the biological medium ( $2.2 \times 10^{-5}$  cm<sup>2</sup>/s) (Santos et al. 2011). If one adds the lack of specific interactions with receptors, it

becomes evident that the understanding of  $\bullet$ NO bioactivity requires the knowledge of its profile of change in time and space, that is, its concentration dynamics. In this context, the use of electrochemical methods associated to carbon fiber microelectrode (micrometer scale) stereotaxically inserted in the CNS is particularly attractive because it allows for real-time and direct detection of  $\bullet$ NO in the the living brain (Barbosa et al. 2008; Lourenço et al. 2011).

The aim of this work was to evaluate the glutamate- $\bullet$ NO signaling pathway in 3 regions of the CNS, namely the hippocampus, the cerebral cortex, and the striatum, in terms of  $\bullet$ NO concentration dynamics, in a rodent model of aging. To this purpose, real-time electrochemical recordings were performed in vivo in the brain of anesthetized Fisher 344 rats (F344) in young, middle- and old-aged animals. We have previously demonstrated that activation of glutamate receptors in these discrete regions in the brain of anesthetized rats results in distinct patterns of  $\bullet$ NO concentration in time and space (Lourenço et al. 2014). Also, age-related changes in the NMDAR- $\bullet$ NO-cGMP pathway appear to be region specific (Jung et al. 2012).

To gain a better understanding of the age-related changes in nitrenergic transmission and neuromodulation, we investigated alterations in the glutamate-evoked  $\bullet$ NO concentrations dynamics in key structures of the CNS. For this purpose, we used modified carbon fiber microelectrodes with high selectivity for  $\bullet$ NO to obtain electrochemical recording of the changes in  $\bullet$ NO concentrations upon brief stimulation of glutamate receptors in the cerebral cortex, striatum, and hippocampus of anesthetized F344 rats at 3 ages (young, middle and old aged). Carbon fiber microelectrodes have been used for several decades for electrochemical detection of chemicals such as catecholamines and  $\bullet$ NO [reviewed in (Budai 2010)]. Modification of the carbon active surface with films such as *o*-phenylenediamine (*o*-PD) and Nafion<sup>®</sup> has been shown to greatly improve sensor analytical performance (Friedemann et al. 1996; Ferreira et al. 2005; Barbosa et al. 2008) and coupled to reduced sensor dimensions (carbon fibers used had an o.d. of 30  $\mu$ m and a tip length of 150–300  $\mu$ m) guarantees high spatial and second-by-second time resolution. Transient production of  $\bullet$ NO was evoked by local applications of a small volume (nL range) of L-glutamate through a glass pipette placed in close proximity to the recording microelectrode, further contributing to high spatial resolution of the recordings obtained. This approach has allowed the recording of  $\bullet$ NO concentration dynamics in slice preparations (Ledo et al. 2004a, 2005, 2010), as well as in vivo in the brain of anesthetized rats (Barbosa et al. 2008; Lourenço et al. 2011; Santos et al. 2011; Lourenço et al. 2014).

## Materials and Methods

### Chemicals and Solutions

Ascorbate (AA), *o*-PD, dopamine, 3,4-dihydroxyphenylacetic acid (DOPAC), 5-hydroxytryptamine (5-HT), and 5-hydroxyindolacetic acid (5-HIAA) were acquired from Sigma. L-glutamate was from Tocris Bioscience. Nafion<sup>®</sup> was from Aldrich. All other reagents were analytical grade. Phosphate buffer saline (0.05 M PBS) used for microelectrodes evaluation was prepared in ultra-pure deionised water ( $R \geq 18.2 \text{ M}\Omega \text{ cm}$ ; Milli-Q, Millipore Integral 10, MA, USA) with the following composition:  $\text{NaH}_2\text{PO}_4$  10 mM;  $\text{Na}_2\text{HPO}_4$  40 mM, NaCl 100 mM, pH 7.4. Saturated  $\bullet\text{NO}$  solution was freshly prepared in ultra-pure deionized water (Milli-Q, Millipore Integral 10, MA, USA) with a resistivity  $\geq 18.2 \text{ M}\Omega \text{ cm}$  previously de-aerated with ultra-pure argon. The solution was prepared by bubbling  $\bullet\text{NO}$  pure gas (commercial cylinder) following sequential passage through NaOH pellets and solution to remove higher oxide contaminants (Barbosa et al. 2011). L-glutamate solution (20 mM) was prepared in NaCl 0.9 %, adjusted to pH 7.4. Prior to filling micropipette for local injection in the brain, each solution was filtered through a sterile syringe filter with  $0.2 \mu\text{m}$  cellulose acetate membrane.

### Animal Groups and Housing

This study was carried out using male F344 rats acquired from Charles River Laboratories (Barcelona, Spain) at the age of 2 months and maintained in the local animal facilities for the period required to achieve target age. Animals were separated into 3 age groups: 6, 12, and 23 months (young, middle and old aged, respectively). A total of 38 animals were used in the present work. The experimental protocol was designed with eight subjects in each age group for the *in vivo* electrochemical recording of  $\bullet\text{NO}$  concentration dynamics. Taking into account expectant loss of animals due to premature death (in accordance to life expectancy chart provided by Charles River Laboratories), at time of acquisition. The young, middle- and old-aged groups were composed of 8, 14 and 16 animals, respectively.

Animals were maintained in a 12:12 light:dark cycle with food and water available *ad libitum*. All experiments were performed in accordance with the European Community Council Directive for the Care and Use of Laboratory Animals (86/609/ECC) and approved by the local institutional animal care committee.

### Behavioral Testing of Memory and Cognitive Decline

The three groups of F344 rats described above were subject to mixed (longitudinal and transversal) behavioral testing. For the behavioral testing, the groups were composed as follows: young age group was composed of 24 male F344 rats at 6 month of age, 8 from each group; the middle-aged group was composed of 22 male F344 rats at 12 month (14 from the middle-aged group and 8 from the old-age group); the old-aged group was composed of 8 male F344 rats at 23 month of age. The open field locomotion test was used to examine motor function by evaluation of spontaneous activity and exploratory behaviors. Animals were allowed to explore an open-field arena ( $75 \times 60 \text{ cm}$ ) for 10 min and the horizontal (free surface movement) and vertical (rearings) exploratory behavior evaluated.

The novel object recognition (NOR) task consisted of habituation, familiarization, and testing was used as a free exploration paradigm to evaluate short-term memory decline. Habituation to the arena was allowed for a 10 min period in the open-field arena ( $75 \times 60 \text{ cm}$ ), in the absence of objects, after which the animal was removed to its holding cage. Familiarization was performed for 5 min in the open-field arena containing 2 identical objects (A + A). Animals were removed from the arena and retained in their cage for a 2 h period prior to final testing. Test was then performed during 5 min in the open-field arena containing 2 objects, one identical to the sample and a novel object (A + B). Time spent exploring each object was measured and the index of NOR was determined as the percentage of time spent exploring the novel object. For both familiarization and test, the objects were placed in opposite and symmetrical corners of the arena.

Spatial memory performance was evaluated using a Plexiglas Y-shaped apparatus consisting of 3 equal arms with a  $120^\circ$  angle between them. In the trial, animals were placed in the Y-maze with one arm blocked and allowed access to the two open arms for 5 min. Animals were removed to their retention cage for a 2 h period prior to test. For the testing, animals were placed back into the maze and allowed access to all 3 arms for 5 min. The percentage of time spent exploring the novel arm in the trial was used as an index of spatial memory performance.

### Carbon Fiber Microelectrodes

Microelectrodes were fabricated as previously described (Santos et al. 2008). Briefly, single carbon fibers ( $30 \mu\text{m}$ , Textron Lowell, MA) were inserted into borosilicate glass capillaries and pulled on a vertical puller. The protruding

carbon fibers were cut to a tip length of 150–300  $\mu\text{m}$ . The electrical contact between the carbon fiber and the copper wire was provided by conductive silver paint. The microelectrodes were tested for their general recording properties in PBS by fast cyclic voltammetry (FCV) at a scan rate of 200 V/s, between  $-1.0$  and  $+1.0$  V vs Ag/AgCl for 30 s (Ensmann Instruments, USA). To improve the analytical properties for in vivo measurements of  $\bullet\text{NO}$ , microelectrodes were coated with two films of Nafion<sup>®</sup> (5 % solution) and electropolymerized with *o*-PD solution (5 mM) at a constant potential of  $+0.7$  V vs Ag/AgCl for 3 periods of 15 min. On the day of experiment, each chemically modified microelectrode was evaluated in terms of sensitivity for  $\bullet\text{NO}$  (using a saturated  $\bullet\text{NO}$  solution) and selectivity against the major interfering analytes in the brain (ascorbic acid, dopamine, serotonin, nitrite) by amperometry at  $+0.9$  V vs Ag/AgCl using a FAST16 high-speed electrochemical system (Quanteon, LLC, Nicholasville, KY, USA) in a two-electrode configuration mode. The modified carbon fiber microelectrodes presented an average sensitivity of  $242.9 \pm 16$  pA/ $\mu\text{M}$  ( $n = 40$ ) and selectivity ratios of 45385:1, 3071:1, 183:1, 441:1, 165:1, and 451:1 against AA ( $n = 40$ ), nitrite ( $n = 39$ ), and dopamine ( $n = 38$ ), DOPAC ( $n = 36$ ), 5-HT ( $n = 36$ ), and 5-HIAA ( $n = 38$ ) respectively.

#### In Vivo Electrochemical Detection of Nitric Oxide in the Rat Brain

The experimental setup used for electrochemical  $\bullet\text{NO}$  detection in vivo was analogous to previous studies (Barbosa et al. 2008; Lourenço et al. 2011; 2014). Briefly, rats were anesthetized with isoflurane 1.5–2 % using an E-Z Anesthesia vaporizer (Braintree Scientific, Inc, USA) and placed in a stereotaxic apparatus. Animal temperature was maintained at 37 °C with a heated pad coupled to a Gaymar Heating Pump (Braintree Scientific, Inc., USA). Craniotomy was performed to expose the desired brain region. Another hole was drilled in a site remote from the recording area for the insertion of an Ag/AgCl reference electrode.

The  $\bullet\text{NO}$  microelectrode was coupled to a micropipette (tip 10–15  $\mu\text{m}$  i.d.) using sticky wax according to a configuration in which tip separation was  $223 \pm 42$   $\mu\text{m}$  ( $n = 30$ ). The micropipette was filled with L-glutamate solution by a syringe fitted with a flexible microfilament (MicroFil, World Precision Instruments, UK).

After removing the dura mater, the microelectrode-micropipette array was inserted into the rat brain regions according to coordinates calculated based on rat brain atlas by Paxinos and Watson (2007). The coordinates for the each region were adjusted for changes in both skull thickness and regional displacement observed with

chronological aging. The existence of major blood vessels on the cortical surface was also considered and adjusted for in each animal. The coordinates used to record  $\bullet\text{NO}$  dynamics in the hippocampus (CA1), calculated from bregma, were AP (antero-posterior)  $-4.1$  to  $-4.2$  mm, ML (medio-lateral)  $-2.2$  to  $-2.4$  mm, and DV (dorso-ventral)  $-2.4$  to  $2.7$  mm. For the striatum, the coordinates used were AP  $+1.2$  to  $2.2$ , ML  $-2.0$  to  $-2.6$ , and DV  $-4.0$  to  $-5.5$  mm. For the measurements performed in the cerebral cortex, coordinates used were AP  $-4.1$  to  $-4.2$ , ML  $-2.0$  to  $-2.2$ , and DV  $-1.7$  to  $-1.8$  mm.

After the insertion of the microelectrode-micropipette array in the brain, the current baseline was allowed to stabilize for at least 30 min. After that period,  $\bullet\text{NO}$  production was stimulated by the pressure ejection of L-glutamate (25 nL) from the micropipette using a Picospritzer III (Parker Hannifin Corp., General Valve Operation, USA).

#### Confirmation of Microelectrode Position

In order to validate the position of the microelectrode in each recording site, at the end of each experiment, a  $+4.5$  V DC current was applied to the carbon fiber microelectrode in order to produce a lesion at the exact recording site in the brain. Animals were then euthanized by cervical displacement under deep anesthesia. The brain was removed and placed in ice-cold freshly prepared 4 % paraformaldehyde in PBS and left to rest at 4 °C for a 24 h period. The brain was then transferred to a 30 % sucrose solution in PBS, for cryopreservation. Once the whole tissue had sunk to the bottom of the sucrose flask, it was considered prepared for cryo-sectioning. Tissue was then frozen with cryospray (Thermo Electron Corporation, UK), and 30  $\mu\text{m}$  coronal sections were cut in a cryostat (ModelCM1900, Leica, Germany). The cryo-sections were then stained with cresyl violet and analyzed under a light microscope to verify the exact location of the recording site. Typical placements of microelectrodes into the cerebral cortex and the CA1 subregion of the hippocampus can be seen in Fig. 1.

#### Data Analysis

The  $\bullet\text{NO}$  signals were characterized in terms of i) peak amplitude of the  $\bullet\text{NO}$  signal, based on the conversion of the amperometric currents to  $\bullet\text{NO}$  fluxes according to Faraday's law ( $I = n.F.\Phi$ , in which  $I$  corresponds to the amperometric current,  $n$  corresponds to the one electron per molecule exchanged for the oxidation of  $\bullet\text{NO}$ , and  $F$  corresponds to the Faraday constant and  $\Phi$  is the flux); ii)  $T_{\text{rise}}$ , the time in seconds required to reach the maximum amplitude after the signal onset, iii)  $T_{\text{decay}}$ , the time in

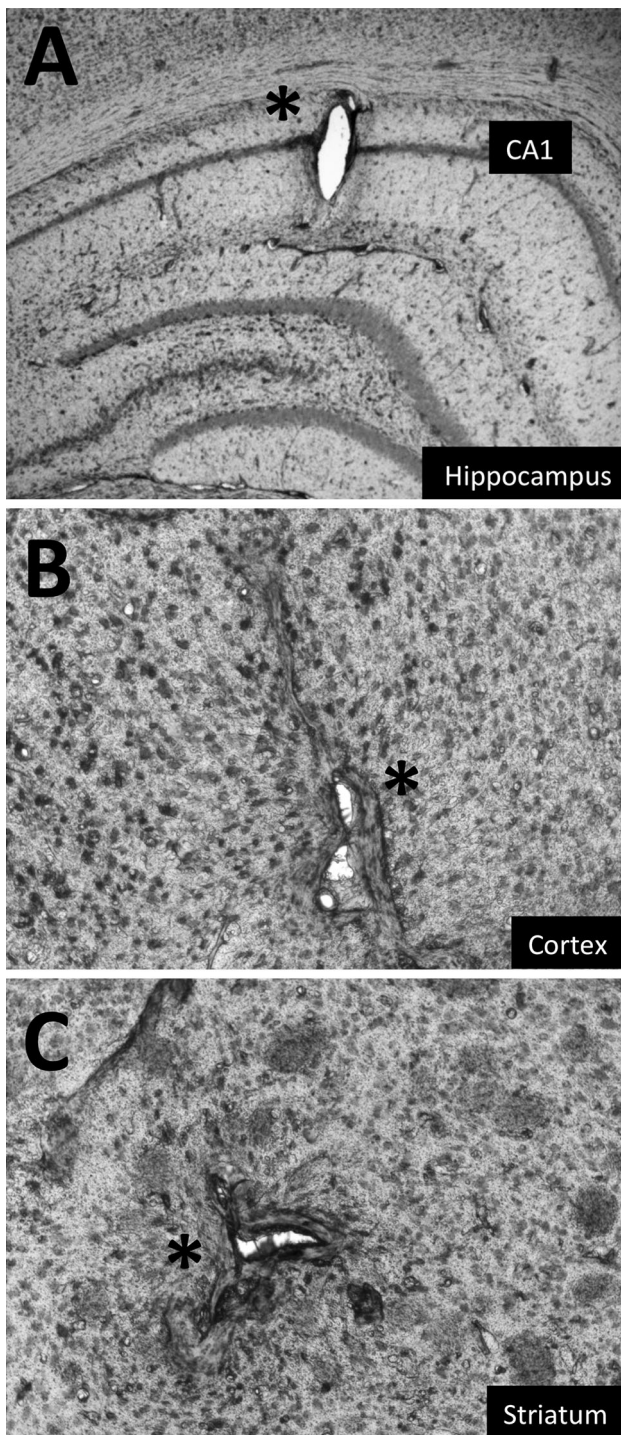


**Fig. 1** Cresyl violet-stained coronal sections of F344 rat brain for confirmation of the microelectrode recording sites (indicated in each photo by the \*) in the different structures of the CNS: the CA1 subregion of the hippocampus (a), the cerebral cortex (b), and the striatum (c)

seconds required to reach 50 % of peak concentration during signal decay, and iv)  $T_{\text{half width}}$  the width at half maximum amplitude. Data are presented as the mean  $\pm$  SEM for the first signal obtained in each region. Statistical

analysis of the data was performed using two-way independent analysis of variance (ANOVA) followed by post hoc Tukey's multiple comparison test to determine differences among regions and age groups. All analyses were performed with GraphPad Prism 5 and Origin 7.5 Software.

## Results

### Behavioral Testing

Age-related alterations in the hippocampal formation in the rodent brain have been shown to associate with decreased performance in behavior tasks that rely on this structure of the temporal medial lobe, such as NOR and Y-maze. The F344 rats used showed age-related decline in cognitive and memory function (Fig. 2), as expected for a model of aging.

The open-field test aimed at evaluating general locomotor activity, revealed a progressive decrease in locomotion and exploratory behavior during aging. With respect to horizontal exploratory behavior, we observed a decrease of 46 and 79 % in middle- and old-aged F344 rats, respectively ( $P < 0.001$ ), relative to young animals (Fig. 2a). This decline in exploratory behavior was recapitulated in the vertical exploratory behavior. The number of rearings of middle- and old-aged animals was, respectively, 46 and 65 % ( $P < 0.05$ ) lower relative to young animal (Fig. 2b). These results suggest a progressive and age-related decrease in locomotor activity in the F344 rats used in the present study.

Novel object recognition and Y-maze tests were performed to assess short-term memory. Analysis of scoring for both tests revealed a tendency for an age-dependent decline in short-term memory function. In the NOR test, middle- and old-aged animals showed a 3 and 23 % decrease, respectively, in % time spent exploring the novel object, when compared to young animals (Fig. 2c). Score for the Y-maze test (evaluated as the % of time spent exploring the novel arm) also showed a 19 and 21 % decrease in middle- and old-aged animals, respectively, when compared to young animals (Fig. 2d).

Since changes in body weight may contribute to performance in behavioral testing, all animals used were weighed prior to testing. For each age group, the average weights were (in g):  $376.2 \pm 4.9$  ( $n = 24$ ) for the young-aged group,  $485.2 \pm 7.2$  ( $n = 22$ ) for the middle-aged group, and  $455 \pm 10.7$  ( $n = 8$ ) for the old-aged group. Both middle- and old-aged animal groups showed significant increase in body mass when compared to young-aged group ( $P < 0.001$ , determined by one-way ANOVA with Tukey's post hoc multiple comparison test). However, the

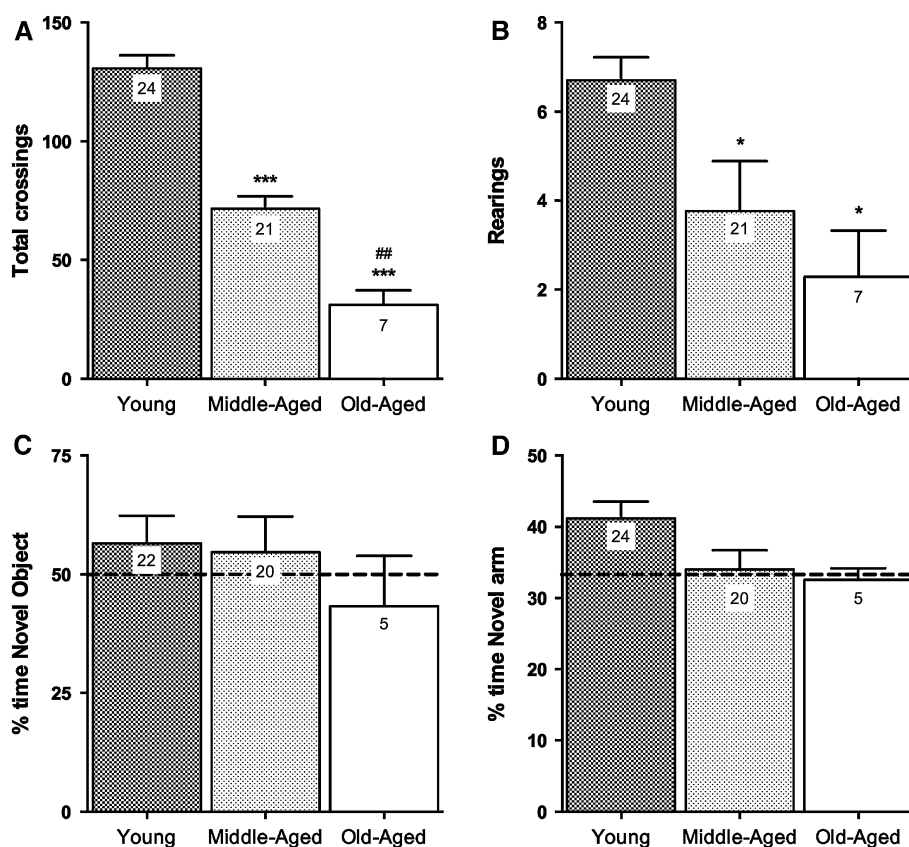


**Fig. 2** Evaluation of age-dependent decline in locomotor activity and short-term memory in the F344 rats. Locomotor activity was assessed by open-field analysis of total number of crossings (a) and total number of rearings (b) observed in the time period of 10 min. Short-term memory was evaluated by performing a novel object recognition test (NOR), where the % of time spent exploring the novel object during the trial phase was determined (c). Animals are expected to spend more than 50 % of time (dashed line) at the novel object. The

Y-maze test was used to evaluate spatial memory, where the % of time spent in the novel arm in the test was determined (d). Animals are expected to spend more than 33 % of time (dashed line) in the novel arm. Bar graphs represent mean  $\pm$  sem. with *N* inset in each bar. \*\*\**P* < 0.0001 and \**P* < 0.005, when compared to young age group; ##*P* < 0.0001 when compared to middle-aged group. Statistical significance determined by one-way Anova with Tukey's post hoc multiple comparison test

old-age group showed a significant decrease in body mass when compared to the middle-aged group (*P* < 0.05).

#### Nitric Oxide Concentration Dynamics in the Central Nervous System

The age-related changes in the glutamate- $\bullet$ NO pathway were evaluated in discrete brain regions of anesthetized F344 rats at different ages. The  $\bullet$ NO concentration dynamics in each region were recorded amperometrically and in real-time, with a second-by-second temporal resolution. Endogenous  $\bullet$ NO production was evoked through activation of glutamatergic transmission via local application of a discrete bolus (in the nanoL range) of a L-glutamate solution (20 mM). The use of carbon fiber microelectrodes of reduced dimensions associated to the geometry of the array containing the stimulation pipette and the recording microelectrode allowed for high spatial resolution to be achieved.

As can be observed in Fig. 3, the same stimulus (L-glutamate, 20 mM) produced distinctive  $\bullet$ NO concentration dynamics in the 3 structures evaluated, the hippocampus, the cerebral cortex and the striatum, both in terms of amplitude and kinetics of signal decay. In the young age group, local stimulation with L-glutamate evoked a transient production of  $\bullet$ NO that, considering the mean maximal  $\bullet$ NO peak, was more robust in the striatum ( $4.76 \pm 1.55$  fmol/s, *n* = 6), followed by the hippocampus ( $4.08 \pm 0.84$  fmol/s, *n* = 6) and finally by the cerebral cortex ( $1.19 \pm 0.59$  fmol/s, *n* = 4). However, the transient  $\bullet$ NO production lasted longer in hippocampus, than in the remaining regions (see Table 1, signal  $T_{\text{half width}}$ ).

In Fig. 4, one can appreciate the age-related changes in  $\bullet$ NO profile in each structure of the CNS. In all the regions, a notorious decrease in  $\bullet$ NO production with age in response to activation of glutamate receptors was observed, in terms of both the amplitude and the duration of the signal. However, such a decrease was more pronounced in the hippocampus

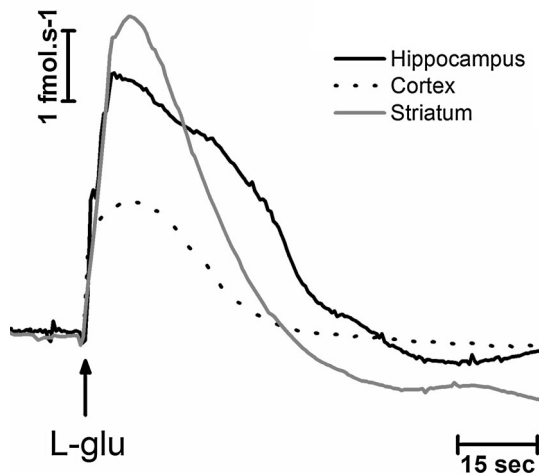


**Fig. 3** Representative electrochemical recording of  $\bullet$ NO concentration dynamics obtained in the hippocampus (filled black line), striatum (filled gray line) and the cerebral cortex (dashed black line) for the young age group upon stimulation of glutamate receptors by locally applying a 25 nL aliquot of L-glutamate (20 mM, indicated with arrow). As seen for the same stimulus paradigm, the  $\bullet$ NO concentration dynamics are distinct amongst the structures of the CNS of the F344 rat

(Fig. 4a) and the striatum (Fig. 4b) as compared with the cortex. Age-dependent decrease in mean maximal flux for  $\bullet$ NO signal can also be appreciated in the bar graph represented in Fig. 5. Two-way analysis of variance of peak  $\bullet$ NO flux revealed that both age and region significantly contribute to observed changes ( $F = 3.24$ ,  $P = 0.046$  and  $F = 6.25$ ,  $P = 0.003$ , respectively), although the 2 factors (age and region tested) showed no interaction ( $F = 0.89$ ,  $P = 0.47$ ). Post hoc Tukey's multiple comparison test further revealed that, for the striatum, peak  $\bullet$ NO flux was significantly decreased in old-aged animals when compared to young and middle-aged subjects ( $P < 0.05$ ). Although statistical

significance of decrease in maximal flux is evident only for the old-aged animal group in the striatum, the tendency for decreasing response in terms of  $\bullet$ NO production upon glutamate receptor activation is evident also in the hippocampus and the cerebral cortex. In old-aged animals, the decrease of the mean maximal flux for  $\bullet$ NO was 73 % in the striatum, 45 % in the cerebral cortex, and 33 % in the hippocampus, relative to the young animals.

## Discussion

In this work, we provide strong evidence that, during chronological age, the glutamate:NMDA receptor:nNOS axis becomes less effective in terms of  $\bullet$ NO production. The role of neuron-produced  $\bullet$ NO in aging has been previously addressed, but this is the first time that this pathway is studied in a direct fashion in vivo. The relevance of such an approach becomes clear if one considers that (1)  $\bullet$ NO conveys information associated to its concentration dynamics and, therefore, the knowledge regarding activity requires the measurement of its profile of change in space and time in a quantitative and direct way and (2) although the distribution of nNOS has been studied by histochemistry of the enzyme, the mere detection in situ does not necessarily imply the presence of active ( $\bullet$ NO producing) enzyme (Lourenço et al. 2014).

Broadly, we found an age-dependent decrease in peak  $\bullet$ NO produced upon stimulation of glutamate receptor activity in the hippocampus, cerebral cortex, and striatum. This decrease in maximal  $\bullet$ NO flux attained was accompanied by a decrease in signal half width, rise time, and decay time in the hippocampus and striatum. Conversely, in the cerebral cortex, all these temporal parameters varied in the opposite direction with age.

**Table 1** Temporal parameters obtained from L-glutamate-evoked  $\bullet$ NO signal recording obtained in the hippocampus, cerebral cortex, and striatum of F344 rats at 3 ages (young, middle and old aged)

		Age		
		Young	Middle Aged	Old Aged
$\frac{1}{2}$ Width, s	Hippocampus	31.8 $\pm$ 3.7 (6)	26.57 $\pm$ 6.7 (7)	26.9 $\pm$ 5.9 (10)
	Cortex	14.5 $\pm$ 5.5 (4)	19.9 $\pm$ 2.8 (8)	36.3 $\pm$ 7.4 (9)*
	Striatum	23.8 $\pm$ 3.2 (6)	16.6 $\pm$ 3.6 (7)	12.3 $\pm$ 3.4 (6)
$T_{\text{rise}}$ , s	Hippocampus	12.2 $\pm$ 2.5 (6)	12.3 $\pm$ 2.8 (11)	6.3 $\pm$ 1.2 (9)
	Cortex	6.8 $\pm$ 1.7 (4)	10 $\pm$ 3.2 (8)	16.6 $\pm$ 4.8 (9)
	Striatum	10.2 $\pm$ 1.7 (6)	8.43 $\pm$ 2.4 (10)	3.8 $\pm$ 0.4 (5)
$T_{\text{decay}}$ , s	Hippocampus	23.3 $\pm$ 4.1 (6)	29.6 $\pm$ 6.2 (11)	20 $\pm$ 4.5 (10)
	Cortex	10.3 $\pm$ 3.8(4)	18.6 $\pm$ 3.0 (9)	24.1 $\pm$ 4.2 (9)
	Striatum	17.2 $\pm$ 1.1 (6)	9.3 $\pm$ 0.7 (6)	9.8 $\pm$ 1.8 (6)

Values in table represent mean  $\pm$  sem ( $n$ ). \*  $P < 0.05$ , evaluated by two-way ANOVA with Tukey's post-test

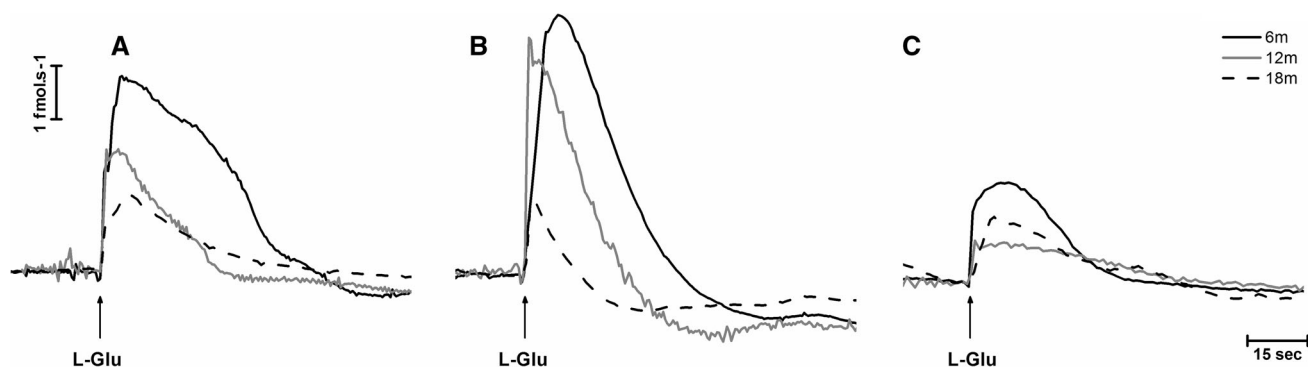


**Fig. 4** Representative recording of  $\bullet$ NO concentration dynamics obtained in the hippocampus (a), striatum (b) and cerebral cortex (c) for the 3 age groups evaluated. In each group of recordings, the filled black line represents the young age group; the filled gray line the

middle-aged group; and the dashed black line the old-aged group. Arrow indicates time of local tissue stimulation by pressure ejection of a 25 nL of L-glutamate (20 mM in saline, pH 7.4) through a glass pipette placed in close proximity to the recording microelectrode

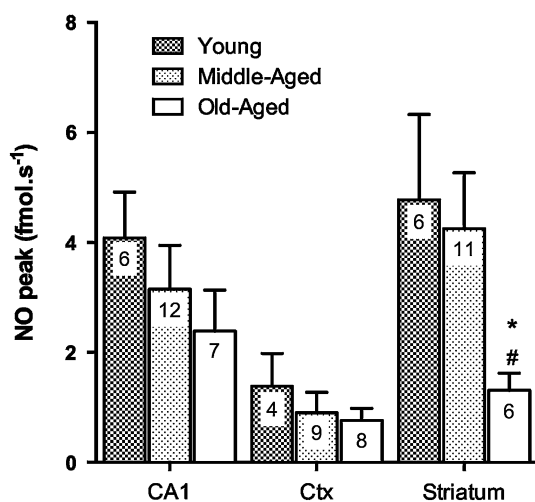


**Fig. 5** Bar graph showing the average peak flux in  $\bullet$ NO obtained in the hippocampus (CA1), cerebral cortex (Ctx), and striatum for the 3 age groups evaluated. Values are represented as mean  $\pm$  sem and number inset each column represents the *N*. \**P* < 0.05 when compared to young group, two-way Anova with Tukey's post-test

In view of these results, the relevance of this pathway for memory and learning rises the hypothesis that the diminished production of neuronal-derived  $\bullet$ NO could translate into decreased cognitive and memory performance.

Accordingly, we observed that the changes in the spatial and temporal pattern of  $\bullet$ NO production were accompanied by age-dependent decline in both general locomotor activity and performance in behavioral testing of short-term and spatial memory. In fact, the attenuation of  $\bullet$ NO signals in the brain areas studied was accompanied by lower scores in behavioral tests performed, such as NOR and Y-maze. These behavioral tests allowed the assessment of short-term and spatial memory in the F344 animal groups, two types of memory that have been linked to hippocampal plasticity. Glutamate-dependent  $\bullet$ NO

production in the brain has been associated with forms of plasticity such as long-term potentiation and depression (LTP and LTD, respectively), two of the neuromolecular correlates of memory and learning. This signaling pathway has been identified in the cerebellum (Jacoby et al. 2001; Shin and Linden 2005; Ogasawara et al. 2007; Qiu and Knopfel 2007), the hippocampus (Garthwaite 2008; Phillips et al. 2008; Taqatqeh et al. 2009) as well as the neocortex (Hardingham et al. 2003; Hardingham and Fox 2006). As such, it is quite interesting to observe that here the decreased scoring in NOR and Y-maze obtained for the old-aged group when compared to young animals, was accompanied by a decrease in glutamate-dependent  $\bullet$ NO production in the CA1 subregion of the hippocampus, a region where LTP is dependent on NMDAr activity, as well as  $\bullet$ NO production (Bliss and Collingridge 1993; Bon and Garthwaite 2003; Hopper and Garthwaite 2006; Bliss and Collingridge 2013).

Extensive literature can be found implicating the medial temporal lobe, in particular the hippocampus, in age-related decline of memory and learning functions. Contradictory reports have shown preserved or decreased neuron count in the hippocampus of aged rats and non-human primates (Driscoll et al. 2006), while others have failed to show a relationship between neuron density and learning deficits (Rasmussen et al. 1996). As such, neuronal loss per se is not likely to fully account for decay in mental function associated with aging, suggesting an association between functional changes in the hippocampus and memory decline.

The circuits found in the neocortex and hippocampus rely upon glutamatergic excitatory transmission, which interacts closely with GABAergic inhibition. The balance between excitatory and inhibitory signaling is fine-tuned by neuromodulators such as  $\bullet$ NO [reviewed in (Feil and Kleppisch 2008)]. The potential for  $\bullet$ NO as a



neuromodulator was first identified in 1988 (Garthwaite et al. 1988) and since then it has been demonstrated to work as a retrograde messenger in several brain structures, namely the hippocampus (Arancio et al. 1996).

Looking into the literature, one finds contradictory reports regarding age-related changes in the neuronal  $\bullet$ NO synthesis pathways in brain structures related to memory. While some studies show age-dependent decrease in NOS-positive neurons, NOS protein, and mRNA levels as well as decrease in L-arginine, L-citrulline, and L-aspartate in several brain regions (Benedetti et al. 1993; Cha et al. 1998; Yu et al. 2000; Necchi et al. 2002; Liu et al. 2009) others point toward age-dependent increase in NOS activity and L-arginine and L-citrulline levels, increased protein and mRNA levels for nNOS and iNOS in the hippocampus and prefrontal cortex and direct association between these increases and impaired memory function in aged rats (Law et al. 2000; Law et al. 2002; Gupta et al. 2012). However, these previous studies provide no information regarding the functional coupling of neuronal activity and  $\bullet$ NO concentration dynamics. In neurons, the nNOS enzyme is physically associated to the NMDAR NR2B subunit via protein–protein interactions mediated by PSD-95 via their respective PDZ domains (Brenman et al. 1996; Christopherson et al. 1999). This assures functional coupling between receptor and enzyme: nNOS requires binding of  $\text{Ca}^{2+}$ -CaM to become active (Alderton et al. 2001) and the NMDAR is typically selectively permeable to  $\text{Ca}^{2+}$  (Paoletti et al. 2013). Taking this into account, and further considering the multiple and complex regulation which nNOS suffers (protein or RNA detection is not a definitive proof of  $\bullet$ NO production), one can easily understand that changes in enzymatic activity, protein or mRNA levels, quantified from neuronal tissue homogenates may not directly translate into changes in neuronal  $\bullet$ NO production.

On the other hand, the physical–chemical nature of  $\bullet$ NO also dictates that distribution and localization of production sites have a high impact on the observed biological activity of this messenger molecule. This small free radical diffuses across cellular compartments and between cells without requiring transporters and/or receptors and, as such, its biological activity is greatly influenced by the distribution and local concentration of molecular targets such as soluble guanylate cyclase, heme and thiol containing proteins, mitochondria, and other radical species (Ledo et al. 2004b; Laranjinha and Ledo 2007; Garthwaite 2008; Thomas et al. 2008; Laranjinha et al. 2012; Heinrich et al. 2013). Once again, determination of total enzyme activity, expression level or mRNA content is unable to provide useful information regarding changes in  $\bullet$ NO bioactivity in a tissue as complex at both the cellular and molecular level as the brain (Lourenço et al. 2014).

Besides nNOS expression, other factors may contribute to shape  $\bullet$ NO concentration profiles during senescence, including regulation and effective coupling to the glutamate pathways or emergence of novel molecular targets in the cellular milieu. In particular, a shift in the intracellular redox status can alter the activity of the NMDAR- and NMDAR-dependent functions, such as plasticity. Recent reports have shown, in middle-aged male F344 rats, a correlation between decrease in acquisition and retention in NMDAR-dependent behavioral tasks and redox-sensitive decrease in NMDAR synaptic transmission (Kumar and Foster 2013). Several cysteine residues on the NMDAR subunits may be sensitive to redox agents, including  $\bullet$ NO, and are thus involved in modulation of NMDAR activity (reviewed in Lipton et al. 2002).

The shift of redox balance observed during senescence may impact  $\bullet$ NO concentration dynamics by providing competing molecular targets such as superoxide radical. These two radicals can combine in a diffusion-limited reaction, yielding the potent oxidant and nitrating agent, peroxynitrite (Koppenol et al. 1992). Increasing levels of intracellular superoxide radical could hypothetically decrease  $\bullet$ NO concentration in the extracellular space and/or contribute to a decrease of its half-life, thus limiting  $\bullet$ NO bioavailability to participate as a neuromodulator in plasticity-associated phenomena. The significance of increases level of oxidants in aging has been recognized (Cui et al. 2012; Kong et al. 2014) and, in the context of the present work, might contribute to the age-related decrease in glutamate-liked  $\bullet$ NO concentration dynamics.

While one may state that these results are in general agreement with those which show decrease in nNOS protein or mRNA levels, or even nNOS activity with age, the results presented here aim to explore the functional coupling between glutamatergic activity and unique concentration dynamics of  $\bullet$ NO in the structures evaluated in the intact and living brain. As such, comparison with other biochemical quantifications obtained in tissue homogenates is difficult to establish.

We previously characterized the different  $\bullet$ NO concentration dynamics coupled to glutamate receptor activation *in vivo* in distinct regions of the CNS of anesthetized Wistar rats (Lourenço et al. 2011, 2014). When comparing the signal parameters obtained in this previous study with the ones obtained here for the young F344 rats, we found a general agreement when considering the peak flux obtained for each region and the following gradient was observed: striatum >hippocampus >cortex, which was also in accordance with our previous findings in young Wistar rats. The same was true for the temporal dynamics, with the hippocampus presenting slower kinetics than the remaining regions.

To the best of our knowledge, the present study provides the first quantitative information of the age-dependent change in the glutamate- $\bullet$ NO signaling pathway in the rodent brain. We report the concentration dynamics of  $\bullet$ NO in the hippocampus (CA1), striatum, and cerebral cortex upon activation of glutamate receptors in young, middle-, and old-aged F344 rats. As previously demonstrated exhaustively (Lourenço et al. 2011, 2014), the observed concentration dynamics were decreased in the presence of the nNOS inhibitor 7-nitroindazole and were not detectable at a working potential of +0.4 V vs Ag/AgCl (data not shown). In sum, the results presented here show a decrease in potency of the glutamate- $\bullet$ NO signaling pathway in all areas of the CNS evaluated, in agreement with decreased performance in behavior testing, suggesting that this particular pathway is indeed critical in maintaining adequate plasticity mechanisms which are subjacent to memory and learning processes, such as LTP. This particular approach which investigates the functional coupling between receptor activation and production patterns of the unique messenger  $\bullet$ NO may potentially allow for a better understanding of the molecular pathways associated with aging when compared to other previous studies which have relied on quantification of enzyme expression levels or activity in tissue homogenates, or even determination of amino-acid precursors of  $\bullet$ NO such as L-arginine. Contrary to these static quantifications, the approach here presented evaluated responsiveness of this particular system, in vivo, in real-time, and with a degree of spatial resolution not achievable by other biochemical methods.

**Acknowledgments** This work was funded by the Portuguese Foundation for Science and Technology (FCT) through the Grants PTDC/SAU-NEU/103538/2008, PEst-C/SAU/LA0001/2011. Lourenço, C.F. acknowledges FCT post-doctoral fellowship SFRH/BPD/82436/2011.

**Conflict of interest** The authors declare no conflict of interest.

## References

- Alderton WK, Cooper CE, Knowles RG (2001) Nitric oxide synthases: structure, function and inhibition. *Biochem J* 357(Pt 3):593–615
- Arancio O, Kiebler M, Lee CJ, Lev-Ram V, Tsien RY, Kandel ER, Hawkins RD (1996) Nitric oxide acts directly in the presynaptic neuron to produce long-term potentiation in cultured hippocampal neurons. *Cell* 87(6):1025–1035
- Barbosa RM, Lourenço CF, Santos RM, Pomerleau F, Huettl P, Gerhardt GA, Laranjinha J (2008) In vivo real-time measurement of nitric oxide in anesthetized rat brain. *Methods Enzymol* 441:351–367. doi:10.1016/s0076-6879(08)01220-2
- Barbosa RM, Lopes Jesus AJ, Santos RM, Pereira CL, Marques CF, Rocha BS, Ferreira NR, Ledo A, Laranjinha J (2011) Preparation, standardization and measurement of nitric oxide solutions. *Glob J Anal Chem* 2(6):272–284
- Benedetti MS, Dostert P, Marrari P, Cini M (1993) Effect of ageing on tissue levels of amino acids involved in the nitric oxide pathway in rat brain. *J Neural Transmission* 94(1):21–30. doi:10.1007/BF01244980
- Benzing WC, Mufson EJ (1995) Increased number of NADPH-d-positive neurons within the substantia innominata in Alzheimer's disease. *Brain Res* 670(2):351–355
- Bishop NA, Lu T, Yankner BA (2010) Neural mechanisms of ageing and cognitive decline. *Nature* 464(7288):529–535. doi:10.1038/nature08983
- Bliss TV, Collingridge GL (1993) A synaptic model of memory: long-term potentiation in the hippocampus. *Nature* 361(6407):31–39. doi:10.1038/361031a0
- Bliss TV, Collingridge GL (2013) Expression of NMDA receptor-dependent LTP in the hippocampus: bridging the divide. *Mol brain* 6:5. doi:10.1186/1756-6606-6-5
- Bon CLM, Garthwaite J (2003) On the role of nitric oxide in hippocampal long-term potentiation. *J Neurosci* 23(5):1941–1948
- Brennan JE, Chao DS, Gee SH, McGee AW, Craven SE, Santillano DR, Wu Z, Huang F, Xia H, Peters MF, Froehner SC, Bredt DS (1996) Interaction of nitric oxide synthase with the postsynaptic density protein PSD-95 and alpha1-syntrophin mediated by PDZ domains. *Cell* 84(5):757–767
- Budai D (2010) Carbon fiber-based microelectrodes and microbiosensors. In: Somerset VS (ed) *Intelligent and Biosensors*. Intech, Croatia, pp 269–288
- Cha CI, Uhm MR, Shin DH, Chung YH, Baik SH (1998) Immunocytochemical study on the distribution of NOS-immunoreactive neurons in the cerebral cortex of aged rats. *NeuroReport* 9(10):2171–2174
- Christopherson KS, Hillier BJ, Lim WA, Bredt DS (1999) PSD-95 assembles a ternary complex with the N-methyl-D-aspartic acid receptor and a bivalent neuronal  $\bullet$ NO synthase PDZ domain. *J Biol Chem* 274(39):27467–27473
- Cui H, Kong Y, Zhang H (2012) Oxidative stress, mitochondrial dysfunction, and aging. *J signal transduct* 2012:646354. doi:10.1155/2012/646354
- Driscoll I, Howard SR, Stone JC, Monfils MH, Tomanek B, Brooks WM, Sutherland RJ (2006) The aging hippocampus: a multi-level analysis in the rat. *Neuroscience* 139(4):1173–1185. doi:10.1016/j.neuroscience.2006.01.040
- Feil R, Kleppisch T (2008) NO/cGMP-dependent modulation of synaptic transmission. *Handb Exp Pharmacol* 184:529–560
- Ferrante RJ, Kowall NW, Beal MF, Richardson EP Jr, Bird ED, Martin JB (1985) Selective sparing of a class of striatal neurons in Huntington's disease. *Science* 230(4725):561–563
- Ferreira N, Ledo A, Frade J, Gerhardt G, Laranjinha J, Barbosa R (2005) Electrochemical measurement of endogenously produced nitric oxide in brain slices using nafion/*o*-phenylenediamine modified carbon fiber microelectrodes. *Anal Chim Acta* 535(1–2):1–7. doi:10.1016/j.aca.2004.12.017
- Friedemann MN, Robinson SW, Gerhardt GA (1996) *o*-Phenylenediamine-modified carbon fiber electrodes for the detection of nitric oxide. *Anal Chem* 68(15):2621–2628
- Garthwaite J (2008) Concepts of neural nitric oxide-mediated transmission. *Eur J Neurosci* 27(11):2783–2802. doi:10.1111/j.1460-9568.2008.06285.x
- Garthwaite J, Charles SL, Chess-Williams R (1988) Endothelium-derived relaxing factor release on activation of NMDA receptors suggests role as intercellular messenger in the brain. *Nature* 336(6197):385–388
- Gupta N, Jing Y, Collie ND, Zhang H, Liu P (2012) Ageing alters behavioural function and brain arginine metabolism in male Sprague-Dawley rats. *Neuroscience* 226:178–196
- Hardingham N, Fox K (2006) The role of nitric oxide and GluR1 in presynaptic and postsynaptic components of neocortical

- potentiation. *J Neurosci* 26(28):7395–7404. doi:[10.1523/JNEUROSCI.0652-06.2006](https://doi.org/10.1523/JNEUROSCI.0652-06.2006)
- Hardingham N, Glazewski S, Pakhotin P, Mizuno K, Chapman PF, Giese KP, Fox K (2003) Neocortical long-term potentiation and experience-dependent synaptic plasticity require alpha-calcium/calmodulin-dependent protein kinase II autophosphorylation. *J Neurosci* 23(11):4428–4436
- Heinrich TA, Dasilva RS, Miranda KM, Switzer CH, Wink DA, Fukuto JM (2013) Biological nitric oxide signaling: chemistry and terminology (\*NO chemical biology and terminology). *Br J Pharmacol* 538(2):120–129
- Hopper RA, Garthwaite J (2006) Tonic and phasic nitric oxide signals in hippocampal long-term potentiation. *J Neurosci* 26(45):11513–11521
- Jacoby S, Sims RE, Hartell NA (2001) Nitric oxide is required for the induction and heterosynaptic spread of long-term potentiation in rat cerebellar slices. *J Physiol* 535(Pt 3):825–839
- Jung J, Na C, Huh Y (2012) Alterations in nitric oxide synthase in the aged CNS. *Oxid Med Cell Longev* 2012:718976. doi:[10.1155/2012/718976](https://doi.org/10.1155/2012/718976)
- Kong Y, Trabucco SE, Zhang H (2014) Oxidative stress, mitochondrial dysfunction and the mitochondria theory of aging. *Interdiscip Top Gerontol* 39:86–107. doi:[10.1159/000358901](https://doi.org/10.1159/000358901)
- Koppenol WH, Moreno JJ, Pryor WA, Ischiropoulos H, Beckman JS (1992) Peroxynitrite, a cloaked oxidant formed by nitric oxide and superoxide. *Chem Res Toxicol* 5(6):834–842
- Kumar A, Foster TC (2013) Linking redox regulation of NMDAR synaptic function to cognitive decline during aging. *J Neurosci* 33(40):15710–15715. doi:[10.1523/JNEUROSCI.2176-13.2013](https://doi.org/10.1523/JNEUROSCI.2176-13.2013)
- Laranjinha J, Ledo A (2007) Coordination of physiologic and toxic pathways in hippocampus by nitric oxide and mitochondria. *Front Biosci* 12:1094–1106. doi:[10.2741/2129](https://doi.org/10.2741/2129)
- Laranjinha J, Santos RM, Lourenço CF, Ledo A, Barbosa RM (2012) Nitric oxide signaling in the brain: translation of dynamics into respiration control and neurovascular coupling. *Ann N Y Acad Sci* 1259(1):10–18
- Law A, Dore S, Blackshaw S, Gauthier S, Quirion R (2000) Alteration of expression levels of neuronal nitric oxide synthase and haem oxygenase-2 messenger RNA in the hippocampi and cortices of young adult and aged cognitively unimpaired and impaired Long-Evans rats. *Neuroscience* 100(4):769–775
- Law A, Gauthier S, Quirion R (2001) Say \*NO to Alzheimer's disease: the putative links between nitric oxide and dementia of the Alzheimer & apos;s type. *Brain Res Brain Res Rev* 35(1):73–96
- Law A, O'Donnell J, Gauthier S, Quirion R (2002) Neuronal and inducible nitric oxide synthase expressions and activities in the hippocampi and cortices of young adult, aged cognitively unimpaired, and impaired long-evans rats. *Neuroscience* 112(2):267–275
- Ledo A, Barbosa RM, Frade J, Laranjinha J (2004a) Nitric oxide monitoring in hippocampal brain slices using electrochemical methods. *Meth Enzymol* 359:111–125
- Ledo A, Frade J, Barbosa RM, Laranjinha J (2004b) Nitric oxide in brain: diffusion, targets and concentration dynamics in hippocampal subregions. *Mol Aspects Med* 25(1–2):75–89. doi:[10.1016/j.mam.2004.02.010](https://doi.org/10.1016/j.mam.2004.02.010)
- Ledo A, Barbosa RM, Gerhardt GA, Cadenas E, Laranjinha J (2005) Concentration dynamics of nitric oxide in rat hippocampal subregions evoked by stimulation of the NMDA glutamate receptor. *Proc Natl Acad Sci USA* 102(48):17483–17488. doi:[10.1073/pnas.0503624102](https://doi.org/10.1073/pnas.0503624102)
- Ledo A, Barbosa R, Cadenas E, Laranjinha J (2010) Dynamic and interacting profiles of \*NO and O<sub>2</sub> in rat hippocampal slices. *Free Radic Biol Med* 48(8):1044–1050. doi:[10.1016/j.freeradbiomed.2010.01.024](https://doi.org/10.1016/j.freeradbiomed.2010.01.024)
- Lipton SA, Choi YB, Takahashi H, Zhang D, Li W, Godzik A, Bankston LA (2002) Cysteine regulation of protein function: as exemplified by NMDA-receptor modulation. *Trends Neurosci* 25(9):474–480
- Liu P, Jing Y, Zhang H (2009) Age-related changes in arginine and its metabolites in memory-associated brain structures. *Neuroscience* 164(2):611–628. doi:[10.1016/j.neuroscience.2009.08.029](https://doi.org/10.1016/j.neuroscience.2009.08.029)
- Lourenço C, Santos R, Barbosa R, Gerhardt G, Cadenas E, Laranjinha J (2011) In vivo modulation of nitric oxide concentration dynamics upon glutamatergic neuronal activation in the hippocampus. *Hippocampus* 21(6):622–630
- Lourenço CF, Ferreira NR, Santos RM, Lukacova N, Barbosa RM, Laranjinha J (2014) The pattern of glutamate-induced nitric oxide dynamics in vivo and its correlation with nNOS expression in rat hippocampus, cerebral cortex and striatum. *Brain Res* 1554:1–11. doi:[10.1016/j.brainres.2014.01.030](https://doi.org/10.1016/j.brainres.2014.01.030)
- Necchi D, Virgili M, Monti B, Contestabile A, Scherini E (2002) Regional alterations of the NO/NOS system in the aging brain: a biochemical, histochemical and immunochemical study in the rat. *Brain Res* 933(1):31–41
- Ogasawara H, Doi T, Doya K, Kawato M (2007) Nitric oxide regulates input specificity of long-term depression and context dependence of cerebellar learning. *PLoS Comput Biol* 3(1):e179. doi:[10.1371/journal.pcbi.0020179](https://doi.org/10.1371/journal.pcbi.0020179)
- Paoletti P, Bellone C, Zhou Q (2013) NMDA receptor subunit diversity: impact on receptor properties, synaptic plasticity and disease. *Nat Publ Group* 14(6):383–400
- Phillips KG, Hardingham NR, Fox K (2008) Postsynaptic action potentials are required for nitric-oxide-dependent long-term potentiation in CA1 neurons of adult GluR1 knock-out and wild-type mice. *J Neurosci* 28(52):14031–14041. doi:[10.1523/JNEUROSCI.3984-08.2008](https://doi.org/10.1523/JNEUROSCI.3984-08.2008)
- Paxinos G, Watson C (2007) *The Rat Brain in Stereotaxic Coordinates* 6th edn. Elsevier Inc., Burlington
- Poon HF, Calabrese V, Scapagnini G, Butterfield DA (2004) Free radicals and brain aging. *Clin Geriatr Med* 20(2):329–359. doi:[10.1016/j.cger.2004.02.005](https://doi.org/10.1016/j.cger.2004.02.005)
- Qiu DL, Knopfel T (2007) An NMDA receptor/nitric oxide cascade in presynaptic parallel fiber-Purkinje neuron long-term potentiation. *J Neurosci* 27(13):3408–3415. doi:[10.1523/JNEUROSCI.4831-06.2007](https://doi.org/10.1523/JNEUROSCI.4831-06.2007)
- Rasmussen T, Schliemann T, Sorensen JC, Zimmer J, West MJ (1996) Memory impaired aged rats: no loss of principal hippocampal and subicular neurons. *Neurobiol Aging* 17(1):143–147
- Santos RM, Lourenço CF, Piedade AP, Andrews R, Pomerleau F, Huettl P, Gerhardt GA, Laranjinha J, Barbosa RM (2008) A comparative study of carbon fiber-based microelectrodes for the measurement of nitric oxide in brain tissue. *Biosens Bioelectron* 24(4):704–709. doi:[10.1016/j.bios.2008.06.034](https://doi.org/10.1016/j.bios.2008.06.034)
- Santos RM, Lourenço CF, Pomerleau F, Huettl P, Gerhardt GA, Laranjinha J, Barbosa RM (2011) Brain nitric oxide inactivation is governed by the vasculature. *Antioxid Redox Signal* 14(6):1011–1021. doi:[10.1089/ars.2010.3297](https://doi.org/10.1089/ars.2010.3297)
- Shin JH, Linden DJ (2005) An NMDA receptor/nitric oxide cascade is involved in cerebellar LTD but is not localized to the parallel fiber terminal. *J Neurophysiol* 94(6):4281–4289. doi:[10.1152/jn.00661.2005](https://doi.org/10.1152/jn.00661.2005)
- Small SA, Tsai WY, DeLaPaz R, Mayeux R, Stern Y (2002) Imaging hippocampal function across the human life span: is memory decline normal or not? *Ann Neurol* 51(3):290–295
- Taqatqeh F, Mergia E, Neitz A, Eysel UT, Koesling D, Mittmann T (2009) More than a retrograde messenger: nitric oxide needs two cGMP pathways to induce hippocampal long-term potentiation. *J Neurosci* 29(29):9344–9350. doi:[10.1523/JNEUROSCI.1902-09.2009](https://doi.org/10.1523/JNEUROSCI.1902-09.2009)

- Thomas DD, Ridnour LA, Isenberg JS, Flores-Santana W, Switzer CH, Donzelli S, Hussain P, Vecoli C, Paolocci N, Ambs S, Colton CA, Harris CC, Roberts DD, Wink DA (2008) The chemical biology of nitric oxide: implications in cellular signaling. *Free Radic Biol Med* 45(1):18–31
- Unger JW, Lange W (1992) NADPH-diaphorase-positive cell populations in the human amygdala and temporal cortex: neuroanatomy, peptidergic characteristics and aspects of aging and Alzheimer's disease. *Acta Neuropathol* 83(6):636–646
- Yu W-J, Juang S-W, Lee J-J, Liu T-P, Cheng J-T (2000) Decrease of neuronal nitric oxide synthase in the cerebellum of aged rats. *Neurosci Lett* 291:37–40